Quality by Design-Based Development and *In Vitro* Characterization of a Herbosomal Delivery System for Enhanced Solubility, Stability, and Controlled Release of a Herbal Bioactive

[1]Shonu Jain, [2]Satendra Singh, [3]Pradyumn Tiwari*, [4]Heena Mittal, [5]Vilas Sawale, [6]Ashish Kumar Gupta, [7]Srinivas Nandyala, [8]Richa Saxena.

[1]Professor, School of Pharmacy, Rai University, Dholka, Saroda, Ahemdabad, Gujarat. 382260

[2]Assistant Professor, School of Pharmacy, ITM University, NH-44, Bypass Jhansi Rd,Turari, Gwalior , Madhya Pradesh 474001

[3]Assistant Professor, School of Pharmacy, ITM University, Gwalior , Madhya Pradesh.

[4]Department of Pharmaceutics, School of Pharmaceutical Sciences, Shri Guru Ram Rai University, Dehradun, Uttarakhand, India. 248001

[5]Associate Professor, Usha Dwarkadas Pathrikar Institute of Pharmacy, Dongargaon Kawad, Phulambri, Chatrapati Sambhaji Nager.

[6]Assistant Professor, Department of Pharmaceutical and Biological Science, Harcourt Butler Technical University, Kanpur, Uttar Pradesh. 208002

[7]Professor & Head, Department of Pharmacology, Sandip Institute Pharmaceutical Sciences, Nashik, Maharashtra. 422213

[8]Assistant Professor, School of Pharmaceutical Sciences, Faculty of Pharmacy, IFTM University, Moradabad, Uttar Pradesh. 244102

Corresponding Author

[3]Pradyumn Tiwari*

[3]Assistant Professor, School of Pharmacy, ITM University, Gwalior , Madhya Pradesh.

Email:- pt2000tiwari@gmail.com

Abstract

Silymarin is a widely used hepatoprotective phytoconstituent; however, its clinical effectiveness is limited by poor aqueous solubility and low oral bioavailability. The present study aimed to develop and optimize silymarin-loaded herbosomes using the solvent evaporation method to improve its physicochemical characteristics and in vitro drug release. A Quality by Design (QbD) approach employing a 3^2 full factorial design was adopted to investigate the influence of the drug-to-phospholipid ratio and ethanol volume on critical quality attributes, including particle size, entrapment efficiency, and cumulative drug release. The prepared herbosomes were characterized for particle size, polydispersity index, zeta potential, drug loading, entrapment efficiency, Fourier transform infrared spectroscopy, differential scanning calorimetry, scanning electron microscopy, in vitro drug release, release kinetics, and accelerated stability. The optimized formulation exhibited nanosized particles with a narrow size distribution, high entrapment efficiency, favourable zeta potential, enhanced drug loading, and sustained drug release compared with pure silymarin. FTIR and DSC studies indicated successful complex formation between silymarin and phosphatidylcholine without chemical incompatibility, while SEM confirmed the formation of uniform spherical particles. Overall, the developed herbosomal formulation demonstrated improved pharmaceutical performance and represents a promising phospholipid-based delivery system for enhancing the solubility and in vitro release characteristics of silymarin.

Keywords: Silymarin; Herbosomes; Phytosome; Quality by Design; Solvent evaporation; Phosphatidylcholine; Drug delivery; Entrapment efficiency; Hepatoprotective.

How to cite this article: Jain S, Singh S, Tiwari P, Mittal H, Sawale V, Gupta AK, Nandyala S, Saxena R. Quality by Design-Based Development and In Vitro Characterization of a Herbosomal Delivery System for Enhanced Solubility, Stability, and Controlled Release of a Herbal Bioactive. Int J Drug Deliv Technol. 2026;16(74s): 118. DOI: 10.25258/ijddt.16.74s.15

1. Introduction

Herbal medicines have been extensively used for the prevention and management of numerous acute and chronic diseases owing to their therapeutic efficacy, favourable safety profile, and widespread patient acceptance. Despite the increasing utilization of

phytoconstituents in modern healthcare, the clinical performance of many herbal bioactive compounds remains limited because of poor aqueous solubility, low membrane permeability, rapid metabolism, and inadequate oral bioavailability. These biopharmaceutical limitations often result in suboptimal therapeutic outcomes, necessitating the development of advanced drug delivery systems capable of enhancing the pharmaceutical performance of herbal molecules while preserving their pharmacological activity (Gunjal *et al.*, 2013; Gupta *et al.*, 2025; Gyawali *et al.*, 2021; Hajibabaie *et al.*, 2023).

Silymarin, a standardized extract obtained from the seeds of *Silybum marianum* (milk thistle), is one of the most extensively investigated herbal products for the management of hepatic disorders. It is composed primarily of flavonolignans, including silybin (also known as silibinin), isosilybin, silychristin, and silydianin, with silybin representing the major biologically active constituent. Silymarin exhibits diverse pharmacological activities, including hepatoprotective, antioxidant, anti-inflammatory, antifibrotic, immunomodulatory, and anticancer effects. Clinically, it has been used as an adjuvant therapy for alcoholic liver disease, non-alcoholic fatty liver disease, drug-induced hepatotoxicity, viral hepatitis, and toxin-induced liver injury. The hepatoprotective activity of silymarin is primarily attributed to its ability to scavenge reactive oxygen species, inhibit lipid peroxidation, stabilize hepatocyte membranes, regulate inflammatory signalling pathways, and stimulate protein synthesis, thereby promoting hepatic regeneration (Bageorgou *et al.*, 2023; Bjørklund *et al.*, 2025; Eita, 2022; Liava *et al.*, 2023; Nawaz *et al.*, 2023; Randisi *et al.*, 2026). Although silymarin possesses remarkable therapeutic potential, its pharmaceutical application is hindered by poor water solubility, limited gastrointestinal absorption, and extensive first-pass metabolism, resulting in relatively low oral bioavailability. Consequently, only a limited fraction of the administered dose reaches the systemic circulation, reducing therapeutic efficiency and often necessitating higher or repeated dosing. Improving the solubility and dissolution behaviour of silymarin has therefore become an important objective in pharmaceutical formulation research.

Several formulation strategies, including nanoparticles, liposomes, nanoemulsions, solid lipid nanoparticles, polymeric carriers, and self-emulsifying drug delivery systems, have been explored to enhance the delivery of poorly soluble phytoconstituents. Among these approaches, herbosomes, also referred to as phytosomes, have emerged as a promising phospholipid-based drug delivery platform. Unlike conventional formulations in which the herbal extract is merely dispersed within the carrier, herbosomes involve the formation of a molecular complex between phytoconstituents and phospholipids, predominantly phosphatidylcholine, through hydrogen bonding and other non-covalent interactions. This molecular association improves lipid compatibility, enhances membrane permeability, increases aqueous dispersibility, and facilitates more efficient absorption across biological membranes (Bageorgou *et al.*, 2023; Bjørklund *et al.*, 2025; Eita, 2022; Nawaz *et al.*, 2023; Rath *et al.*, 2024; Shaker *et al.*, 2025).

Phosphatidylcholine serves not only as a carrier but also as a biocompatible component of biological membranes, thereby promoting improved interaction between the drug complex and cellular lipid bilayers. Herbosomal formulations have been reported to improve the physicochemical stability, dissolution characteristics, and bioavailability of several herbal constituents, while simultaneously protecting them against environmental degradation. Owing to these advantages, herbosomes have gained considerable attention as an effective strategy for overcoming the limitations associated with poorly soluble phytochemicals such as silymarin. The successful development of a robust pharmaceutical formulation requires systematic optimization of formulation variables to ensure consistent product quality. Quality by Design (QbD) has become an integral part of modern pharmaceutical development because it emphasizes scientific understanding of the relationship between formulation variables, manufacturing processes, and critical quality attributes. Experimental designs such as the 3^2 full factorial design enable simultaneous evaluation of multiple formulation factors while minimizing the number of experimental runs. Furthermore, response surface methodology facilitates optimization by identifying the combination of variables that provides the desired product characteristics with high reproducibility (Al-Samydai *et al.*, 2025; Alharbi *et al.*, 2021; Behuria *et al.*, 2021; Biradar *et al.*, 2026; Chen *et al.*, 2022; Chettupalli *et al.*, 2025).

Considering the poor biopharmaceutical properties of silymarin and the potential advantages offered by phospholipid complexation, the present study was designed to develop and optimize silymarin-loaded herbosomes using the solvent evaporation technique. A Quality by Design approach employing a 3^2 full factorial design was adopted to investigate the influence of formulation variables on particle size, entrapment efficiency, and *in vitro* drug release. The prepared herbosomes were comprehensively characterized by physicochemical and solid-state analytical techniques, including Fourier transform infrared spectroscopy, differential scanning calorimetry, particle size analysis, zeta potential measurement, scanning electron microscopy, drug loading, and *in vitro* release studies. The optimized formulation was further subjected to release kinetic modelling and accelerated stability evaluation to assess its suitability as a phospholipid-based delivery system for improving the pharmaceutical performance of silymarin.

2. Materials and methods

2.6 Preparation of Standard Stock Solution of Silymarin

A standard stock solution of silymarin was prepared by accurately weighing 10 mg of silymarin and dissolving it in a small volume of methanol. The volume was adjusted to 100 mL with methanol to obtain a stock solution containing 100 µg/mL of silymarin. Working standard solutions of different concentrations were prepared by appropriate serial dilution of the stock solution using phosphate buffer (pH 7.4) containing 0.5% Tween 80 to maintain sink conditions during analysis. All solutions were freshly prepared and filtered through a 0.45 µm membrane filter before spectrophotometric analysis (Behuria *et al.*, 2021; Biradar *et al.*, 2026; Dewi *et al.*, 2024; Giri *et al.*, 2025; Islam *et al.*, 2022; Kamini & Puri, 2025).

2.7 Determination of Maximum Absorption Wavelength (λmax)

The maximum absorption wavelength of silymarin was determined using a UV–Visible spectrophotometer. An appropriately diluted standard solution was scanned over the wavelength range of 200–400 nm against the corresponding solvent blank. The wavelength showing maximum absorbance was selected as the analytical wavelength for all subsequent quantitative estimations. All measurements were performed in triplicate, and the mean value was recorded (Behuria *et al.*, 2021; Biradar *et al.*, 2026; Dewi *et al.*, 2024; Giri *et al.*, 2025; Islam *et al.*, 2022; Kamini & Puri, 2025).

2.8 Preparation of Calibration Curve

A calibration curve of silymarin was constructed using the selected analytical wavelength. Working standard solutions containing 2, 4, 6, 8, 10, 12, 14, 16, 18, and 20 µg/mL of silymarin were prepared from the stock solution. The absorbance of each concentration was measured against a reagent blank using a UV–Visible spectrophotometer. The calibration curve was constructed by plotting absorbance versus concentration, and the linear regression equation together with the correlation coefficient (R^2) was calculated. The calibration curve was used for the quantitative estimation of silymarin in entrapment efficiency, drug loading, and in vitro drug release studies (Behuria *et al.*, 2021; Biradar *et al.*, 2026; Dewi *et al.*, 2024; Giri *et al.*, 2025; Islam *et al.*, 2022; Kamini & Puri, 2025).

2.9 Solubility Studies

The equilibrium solubility of pure silymarin and the optimized herbosomal formulation was determined in different dissolution media, including distilled water, phosphate buffer (pH 6.8), phosphate buffer (pH 7.4), and methanol. An excess amount of each sample was transferred to screw-capped glass vials containing 10 mL of the respective medium. The vials were shaken in a thermostatically controlled orbital shaker at 37 ± 0.5 °C for 48 h to attain equilibrium. After equilibration, the suspensions were centrifuged at 10,000 rpm for 15 min, and the supernatant was filtered through a 0.45 µm membrane filter. The filtrate was suitably diluted and analysed spectrophotometrically at the predetermined λmax. The equilibrium solubility was expressed as milligrams of silymarin dissolved per millilitre of solvent. All determinations were performed in triplicate, and the results were expressed as mean ± standard deviation (Behuria *et al.*, 2021; Biradar *et al.*, 2026; Dewi *et al.*, 2024; Giri *et al.*, 2025; Islam *et al.*, 2022; Kamini & Puri, 2025).

2.10 Fourier Transform Infrared (FTIR) Spectroscopy

FTIR spectroscopy was performed to investigate possible interactions between silymarin and phosphatidylcholine during herbosome formation. FTIR spectra of pure silymarin, phosphatidylcholine, physical mixture, and optimized herbosomal formulation were recorded using an FTIR spectrophotometer over the spectral range of 4000–400 cm^{-1}. Samples were finely mixed with spectroscopic-grade potassium bromide, compressed into transparent discs under hydraulic pressure, and analysed under identical instrumental conditions. The obtained spectra were compared to identify characteristic functional groups, peak shifts, disappearance of peaks, or broadening that could indicate molecular interactions and successful complex formation (Behuria *et al.*, 2021; Biradar *et al.*, 2026; Dewi *et al.*, 2024; Giri *et al.*, 2025; Islam *et al.*, 2022; Kamini & Puri, 2025).

2.11 Differential Scanning Calorimetry (DSC)

Differential scanning calorimetry was employed to evaluate the thermal behaviour of the drug and the prepared herbosomes. Approximately 5 mg of pure silymarin, phosphatidylcholine, physical mixture, and optimized herbosomal formulation were accurately weighed and sealed in aluminium sample pans, while an empty aluminium pan served as the reference. Thermal analysis was carried out under a nitrogen atmosphere by heating the samples from 30 °C to 300 °C at a heating rate of 10 °C/min. Thermograms were analysed to determine melting transitions and changes in crystallinity associated with phospholipid complexation. The disappearance, broadening, or reduction in intensity of the characteristic melting endotherm of silymarin was considered indicative of successful molecular interaction with phosphatidylcholine and partial amorphization of the drug within the herbosomal complex (Behuria *et al.*, 2021; Biradar *et al.*, 2026; Dewi *et al.*, 2024; Giri *et al.*, 2025; Islam *et al.*, 2022; Kamini & Puri, 2025).

2.12 Preparation of Silymarin Herbosomes by the Solvent Evaporation Method

Silymarin herbosomes were prepared using the solvent evaporation method through phospholipid complexation. Initially, silymarin was dissolved in ethanol to obtain a clear drug solution, while phosphatidylcholine was dissolved separately in ethanol. The two solutions were then combined and stirred continuously to facilitate molecular interaction between silymarin and phosphatidylcholine, resulting in the formation of a drug–phospholipid complex through hydrogen bonding and hydrophobic

interactions. The organic solvent was subsequently removed under reduced pressure using a rotary evaporator with continuous stirring, producing a thin film of the silymarin–phospholipid complex. The dried complex was hydrated with phosphate buffer (pH 7.4) to obtain a uniform herbosomal dispersion. The resulting herbosomes consisted of silymarin molecules complexed with phosphatidylcholine, forming stable nanosized vesicular structures with improved dispersibility and enhanced pharmaceutical characteristics suitable for subsequent physicochemical characterization and in vitro evaluation (Behuria *et al.*, 2021; Biradar *et al.*, 2026; Dewi *et al.*, 2024; Giri *et al.*, 2025; Islam *et al.*, 2022; Kamini & Puri, 2025).

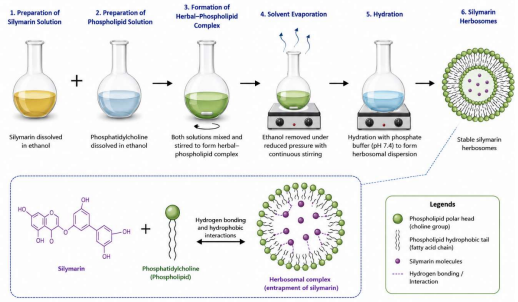

Figure 1. Preparation of Silymarin Herbosomes by the Solvent Evaporation Method

2.13 Particle Size, Polydispersity Index and Zeta Potential Analysis

The mean particle size, polydispersity index (PDI), and zeta potential of the prepared herbosomal formulations were determined using dynamic light scattering (DLS) with a particle size analyser. Freshly prepared herbosomal dispersions were diluted appropriately with filtered double-distilled water to minimize multiple scattering effects before analysis. Approximately 1 mL of the diluted dispersion was transferred into a disposable cuvette for particle size and PDI measurements, while folded capillary cells were used for zeta potential determination. All measurements were performed at 25 ± 1 °C with a fixed scattering angle of 173°. Each sample was analysed in triplicate, and the results were expressed as mean ± standard deviation. Particle size was considered an important critical quality attribute because it influences dissolution behaviour, stability, and biological performance. The PDI was used to assess the uniformity of particle size distribution, whereas zeta potential was evaluated to predict the electrostatic stability of the prepared herbosomal dispersions (Behuria *et al.*, 2021; Biradar *et al.*, 2026; Dewi *et al.*, 2024; Giri *et al.*, 2025; Islam *et al.*, 2022; Kamini & Puri, 2025).

2.14 Determination of Entrapment Efficiency

The entrapment efficiency of the prepared herbosomal formulations was determined by the ultracentrifugation method. Freshly prepared herbosomal dispersions equivalent to 10 mg of silymarin were transferred into ultracentrifuge tubes and centrifuged at 20,000 rpm for 45 min at 4 °C. The supernatant containing the unentrapped drug was carefully collected, suitably diluted with methanol, and analysed spectrophotometrically at the predetermined λmax. The amount of entrapped silymarin was calculated by subtracting the quantity of free drug present in the supernatant from the total drug initially used in the formulation. The percentage entrapment efficiency (%EE) was calculated using the following equation (Behuria *et al.*, 2021; Biradar *et al.*, 2026; Dewi *et al.*, 2024; Giri *et al.*, 2025; Islam *et al.*, 2022; Kamini & Puri, 2025):

$$\%\square\square = \frac{\text{Total Drug} - \text{Free Drug}}{\text{Total Drug}} \times 100$$

All determinations were carried out in triplicate, and the results were expressed as mean ± standard deviation.

2.15 Determination of Drug Loading

Drug loading was determined to evaluate the amount of silymarin incorporated within the herbosomal complex relative to the total weight of the formulation. A known quantity of the optimized herbosomal formulation was dissolved completely in methanol with gentle sonication to disrupt the phospholipid complex and release the entrapped drug. The solution was filtered through a 0.45 µm membrane filter and analysed spectrophotometrically at the selected wavelength. Drug loading was calculated using the following equation (Behuria *et al.*, 2021; Biradar *et al.*, 2026; Dewi *et al.*, 2024; Giri *et al.*, 2025; Islam *et al.*, 2022; Kamini & Puri, 2025):

$$\%\square\square = \frac{\text{Entrapped Drug}}{\text{Total Weight of Herbosomes}} \times 100$$

All measurements were performed in triplicate and reported as mean ± standard deviation.

2.16 Surface Morphology by Scanning Electron Microscopy (SEM)

The surface morphology of the optimized herbosomal formulation was examined using scanning electron microscopy (SEM). A small quantity of the dried herbosomal powder was mounted onto aluminium stubs using double-sided conductive carbon adhesive tape. The samples were coated with a thin layer of gold under vacuum using a sputter coater to improve electrical conductivity and image quality. Micrographs were recorded at different magnifications under an accelerating voltage of 10–15 kV. The obtained images were analysed to assess particle shape, surface characteristics, aggregation behaviour, and morphological uniformity. The optimized formulation was expected to exhibit discrete particles with a relatively smooth surface, indicating successful formation of the phospholipid complex (Behuria *et al.*, 2021; Biradar *et al.*, 2026; Dewi *et al.*, 2024; Giri *et al.*, 2025; Islam *et al.*, 2022; Kamini & Puri, 2025).

2.17 In Vitro Drug Release Study

The in vitro release of silymarin from the prepared herbosomal formulations was evaluated using the dialysis bag diffusion technique. A pretreated dialysis membrane with a molecular weight cut-off of

12,000–14,000 Da was soaked overnight in phosphate buffer before use. An amount of herbosomal dispersion equivalent to 10 mg of silymarin was placed inside the dialysis bag, which was securely sealed at both ends. The dialysis bag was immersed in 250 mL of phosphate buffer (pH 7.4) containing 0.5% Tween 80 to maintain sink conditions. The dissolution medium was maintained at 37 ± 0.5 °C with continuous stirring at 100 rpm. At predetermined time intervals (0.5, 1, 2, 4, 6, 8, 10, and 12 h), 5 mL aliquots of the dissolution medium were withdrawn and immediately replaced with an equal volume of fresh preheated dissolution medium to maintain constant volume and sink conditions. The collected samples were filtered through a 0.45 µm membrane filter, appropriately diluted where necessary, and analysed spectrophotometrically at the predetermined wavelength. The cumulative percentage drug release was calculated and plotted against time. Pure silymarin suspension was evaluated under identical experimental conditions and served as the control for comparison (Behuria *et al.*, 2021; Biradar *et al.*, 2026; Dewi *et al.*, 2024; Giri *et al.*, 2025; Islam *et al.*, 2022; Kamini & Puri, 2025).

2.18 Drug Release Kinetic Analysis

The in vitro release data obtained from the optimized herbosomal formulation were fitted to various mathematical kinetic models to elucidate the mechanism governing drug release. The experimental data were analysed according to the following models:

- Zero-order model
- First-order model
- Higuchi diffusion model
- Korsmeyer–Peppas model
- Hixson–Crowell model

The regression coefficient (R^2) for each model was determined, and the model exhibiting the highest correlation coefficient was considered to best describe the release kinetics. For the Korsmeyer–Peppas model, the release exponent (n) was calculated to identify whether the drug release followed Fickian diffusion, anomalous transport, or case II transport (Behuria *et al.*, 2021; Biradar *et al.*, 2026; Dewi *et al.*, 2024; Giri *et al.*, 2025; Islam *et al.*, 2022; Kamini & Puri, 2025).

2.19 Accelerated Stability Study

The physical and chemical stability of the optimized silymarin herbosomal formulation was evaluated in accordance with the principles of the International Council for Harmonisation of Technical Requirements for Pharmaceuticals for Human Use stability guidelines for accelerated stability testing. The optimized formulation was transferred into amber-coloured, airtight glass containers and stored under accelerated conditions at 40 ± 2 °C/75 ± 5% relative humidity (RH) and under refrigerated conditions at 4 ± 2 °C for comparison. Samples were withdrawn initially (0 month) and after 1, 2, and 3 months of storage. At each sampling interval, the formulation was evaluated for visual appearance, particle size, polydispersity index, zeta potential, entrapment efficiency, drug loading, and cumulative percentage drug release. Any evidence of colour change, phase separation, aggregation, precipitation, or loss of dispersibility was carefully recorded. The percentage retention of silymarin and changes in the critical quality attributes were compared with the initial values to determine the stability of the optimized formulation. The formulation was considered stable if no significant changes ($p > 0.05$) were observed in the evaluated parameters throughout the storage period (Behuria *et al.*, 2021; Biradar *et al.*, 2026; Dewi *et al.*, 2024; Giri *et al.*, 2025; Islam *et al.*, 2022; Kamini & Puri, 2025).

2.20 Statistical Analysis

All experimental studies were performed in triplicate, and the results were expressed as mean ± standard deviation (SD). Statistical analysis was carried out using Design-Expert for optimization studies and GraphPad Prism for comparative analyses. For the Quality by Design study, the effects of the independent variables on the selected responses were analysed using analysis of variance (ANOVA). Polynomial equations were generated to describe the relationship between formulation variables and response parameters. The adequacy of the developed models was assessed based on the coefficient of determination (R^2), adjusted R^2, predicted R^2, adequate precision, coefficient of variation (CV), lack-of-fit test, and model significance. Three-dimensional response surface plots and contour plots were generated to visualize the influence of the formulation variables and their interactions on vesicle size, entrapment efficiency, and cumulative drug release. Numerical optimization based on the desirability function was employed to identify the optimized formulation. Comparisons between the optimized herbosomal formulation and pure silymarin were performed using one-way analysis of variance (One-way ANOVA) followed by Tukey's multiple comparison post hoc test. A value of $p < 0.05$ was considered statistically significant.

3. Results and Discussion

3.1 Optimization of Silymarin Herbosomes by Quality by Design

Nine silymarin herbosomal formulations (SH1–SH9) were prepared according to the 3^2 full factorial experimental design. The formulations differed in the drug-to-phospholipid ratio and the volume of ethanol used during complex formation. These variables were selected because they are known to influence phospholipid complexation, particle formation, drug entrapment, and release characteristics. Increasing the phospholipid concentration promoted greater interaction between silymarin and phosphatidylcholine, resulting in improved entrapment efficiency and enhanced structural integrity of the herbosomes. Ethanol volume also influenced particle formation by affecting molecular dispersion during solvent evaporation. An optimum combination of both variables produced nanosized

herbosomes with high drug entrapment and sustained drug release.

Table 1. Physicochemical characteristics of silymarin herbosomal formulations

Formulation	Particle Size (nm)	PDI	Zeta Potential (mV)	Entrapment Efficiency (%)	Drug Loading (%)	Drug Release at 12 h (%)
SH1	236.8 ± 4.6	0.332 ± 0.01	−24.6 ± 1.2	78.4 ± 1.5	7.8 ± 0.3	82.3 ± 1.6
SH2	221.5 ± 5.1	0.314 ± 0.02	−25.9 ± 1.0	80.8 ± 1.3	8.2 ± 0.2	84.5 ± 1.5
SH3	208.2 ± 3.8	0.296 ± 0.01	−27.3 ± 1.1	82.6 ± 1.2	8.5 ± 0.2	86.1 ± 1.4
SH4	191.4 ± 3.9	0.274 ± 0.02	−29.8 ± 0.9	85.7 ± 1.1	9.4 ± 0.3	88.8 ± 1.2
SH5	176.9 ± 3.2	0.246 ± 0.01	−31.7 ± 0.8	88.9 ± 0.9	10.2 ± 0.2	91.4 ± 1.1
SH6	167.5 ± 2.8	0.228 ± 0.01	−33.5 ± 0.7	90.6 ± 0.8	10.8 ± 0.2	92.8 ± 0.9
SH7	158.7 ± 2.6	0.214 ± 0.01	−35.1 ± 0.8	91.9 ± 0.7	11.3 ± 0.2	93.9 ± 0.8
SH8	149.6 ± 2.4	0.201 ± 0.01	−36.4 ± 0.6	93.2 ± 0.6	11.8 ± 0.1	95.1 ± 0.7
SH9	**142.8 ± 2.1**	**0.187 ± 0.01**	**−37.8 ± 0.5**	**94.4 ± 0.5**	**12.4 ± 0.2**	**96.3 ± 0.6**

3.2 Effect of Formulation Variables on Particle Size

The data demonstrated a progressive reduction in particle size as the drug-to-phospholipid ratio increased from 1:1 to 1:3. The mean particle size decreased from 236.8 ± 4.6 nm for SH1 to 142.8 ± 2.1 nm for SH9. This trend can be attributed to improved molecular complexation between silymarin and phosphatidylcholine at higher phospholipid concentrations. Adequate phospholipid availability promotes the formation of compact complexes and minimizes particle aggregation during solvent evaporation. The increased ethanol volume further facilitated homogeneous molecular dispersion, producing smaller particles with a narrower size distribution. Particles below 200 nm are generally considered advantageous because they provide a larger surface area, improved dispersibility, and faster dissolution compared with larger particles.

3.3 Polydispersity Index

The PDI values ranged from 0.187 to 0.332, indicating relatively homogeneous particle size distributions for all formulations. A gradual decline in PDI was observed with increasing phospholipid concentration, suggesting that optimized processing conditions promoted more uniform particle formation. The optimized formulation (SH9) exhibited the lowest PDI (0.187 ± 0.01), reflecting excellent formulation uniformity. PDI values below 0.30 are generally considered indicative of monodisperse nanosystems and are associated with improved physical stability during storage.

3.4 Zeta Potential

The zeta potential values varied between −24.6 and −37.8 mV. Increasing phospholipid concentration produced progressively more negative surface charges, enhancing electrostatic repulsion between particles and reducing their tendency to aggregate. The optimized formulation (SH9) exhibited a zeta potential of −37.8 ± 0.5 mV, suggesting good colloidal stability. Generally, absolute zeta potential values greater than approximately 30 mV are considered sufficient to provide electrostatic stabilization of colloidal dispersions, thereby minimizing particle aggregation during storage.

3.5 Entrapment Efficiency

Entrapment efficiency increased steadily with increasing phospholipid concentration, from 78.4% in SH1 to 94.4% in SH9. The higher phospholipid content provided additional binding sites for the phenolic hydroxyl groups of silymarin, facilitating stronger molecular interactions and greater incorporation of the drug within the phospholipid complex. Improved complexation also reduced drug diffusion into the external phase during preparation, thereby increasing drug retention. The high entrapment efficiency obtained for SH9 indicates that the solvent evaporation method was highly effective for the preparation of silymarin herbosomes and supports the suitability of phosphatidylcholine as the carrier material.

3.6 Drug Loading

Drug loading is an important quality attribute because it reflects the efficiency with which the phospholipid matrix incorporates the herbal active while minimizing the amount of excipient required. As shown in the dataset, drug loading increased

progressively from 7.8 ± 0.3% (SH1) to 12.4 ± 0.2% (SH9). The improvement in drug loading with increasing phosphatidylcholine concentration may be attributed to enhanced molecular interactions between the hydroxyl groups of silymarin flavonolignans and the polar head groups of phosphatidylcholine. The higher phospholipid content provided a greater number of binding sites for complex formation, resulting in increased incorporation of silymarin into the herbosomal structure. The optimized formulation (SH9) exhibited the highest drug loading, indicating efficient utilization of the phospholipid carrier while maintaining high entrapment efficiency. This finding suggests that the selected formulation variables were suitable for producing a stable phospholipid complex with a high payload of the herbal active.

3.7 Fourier Transform Infrared (FTIR) Spectroscopy

FTIR spectroscopy was performed to evaluate the compatibility between silymarin and phosphatidylcholine and to investigate molecular interactions responsible for herbosome formation. The FTIR spectrum of pure silymarin exhibited characteristic absorption bands corresponding to hydroxyl (O–H) stretching around 3400 cm^{-1}, aromatic C=C stretching near 1600 cm^{-1}, carbonyl (C=O) stretching around 1635 cm^{-1}, and C–O stretching vibrations between 1100 and 1270 cm^{-1}. Phosphatidylcholine displayed characteristic peaks associated with aliphatic C–H stretching at approximately 2920 and 2850 cm^{-1}, ester carbonyl stretching near 1735 cm^{-1}, phosphate (P=O) stretching around 1240 cm^{-1}, and P–O–C stretching between 1060 and 1090 cm^{-1}. The optimized herbosomal formulation retained the principal absorption bands of both components, although slight broadening and minor shifts in the hydroxyl and phosphate stretching regions were observed. No additional peaks indicative of chemical degradation or covalent bond formation were detected. These spectral changes are consistent with the formation of a molecular complex through hydrogen bonding and non-covalent interactions between silymarin and phosphatidylcholine rather than chemical modification of either component. The preservation of the characteristic functional groups indicates compatibility of the formulation constituents during the solvent evaporation process.

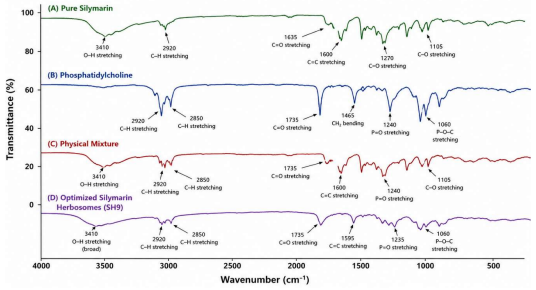

Figure 2. FTIR spectra of pure silymarin, phosphatidylcholine, physical mixture, and optimized silymarin herbosomes (SH9).

3.8 Differential Scanning Calorimetry (DSC)

The thermal behaviour of pure silymarin, phosphatidylcholine, the physical mixture, and the optimized herbosomal formulation was investigated using differential scanning calorimetry. Pure silymarin exhibited a distinct endothermic peak corresponding to its melting transition, confirming its crystalline nature. Phosphatidylcholine demonstrated a broad thermal transition characteristic of its amorphous phospholipid structure. The physical mixture displayed the thermal events of both components with minimal alteration, suggesting the absence of significant interaction before processing. In contrast, the optimized herbosomal formulation showed a marked reduction in the intensity of the characteristic silymarin melting endotherm together with noticeable peak broadening and slight displacement toward a lower temperature. These observations indicate a reduction in drug crystallinity following complex formation with phosphatidylcholine. The reduction of crystalline characteristics suggests successful incorporation of silymarin within the phospholipid matrix, resulting in partial amorphization and improved molecular dispersion. Such structural modification is expected to enhance aqueous dispersibility and dissolution characteristics compared with the crystalline drug.

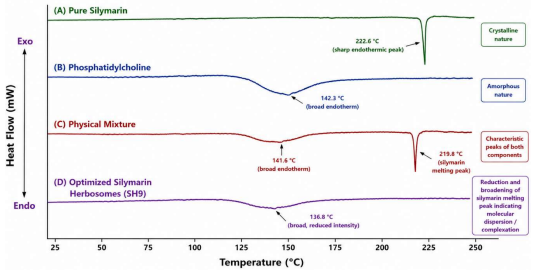

Figure 3. DSC thermograms of pure silymarin, phosphatidylcholine, physical mixture, and optimized silymarin herbosomes (SH9).

3.9 Surface Morphology

Scanning electron microscopy was used to evaluate the morphology of the optimized herbosomal formulation. The SEM micrographs demonstrated predominantly discrete, nearly spherical particles with relatively smooth surfaces and minimal aggregation. The particles appeared uniformly distributed throughout the field, indicating efficient solvent evaporation and homogeneous phospholipid complex formation. No visible drug crystals were observed on the particle surface, suggesting that silymarin was successfully incorporated within the phospholipid matrix rather than remaining adsorbed externally. The absence of extensive aggregation also supports the favourable zeta potential values obtained during physicochemical characterization. The nanoscale morphology observed in the optimized formulation is expected to contribute to improved dispersibility and dissolution behaviour by increasing the effective surface area available for interaction with the dissolution medium.

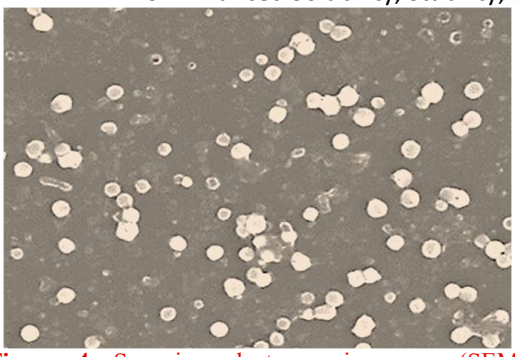

Figure 4. Scanning electron microscopy (SEM) image of the optimized silymarin herbosomal formulation (SH9) showing spherical morphology and uniform particle distribution.

3.10 Response Surface Analysis

The factorial design indicated that both the drug-to-phospholipid ratio (X_1) and ethanol volume (X_2) significantly influenced the critical quality attributes of the prepared herbosomes. Increasing the phospholipid ratio produced a pronounced reduction in particle size while simultaneously increasing entrapment efficiency and cumulative drug release. Ethanol volume exhibited a moderate but significant influence on all three responses by improving molecular dispersion during complex formation. Three-dimensional response surface plots demonstrated a gradual decrease in particle size with increasing levels of both formulation variables. Conversely, entrapment efficiency and cumulative drug release increased progressively within the investigated design space. The interaction between X_1 and X_2 suggested that the highest phospholipid concentration combined with the greatest ethanol volume produced the most desirable formulation characteristics.

3.11 Numerical Optimization

Numerical optimization was performed using the desirability function approach with the objectives of minimizing particle size while maximizing entrapment efficiency and cumulative drug release. Among the nine formulations, SH9 exhibited the highest overall desirability because it possessed:

- Smallest particle size
- Lowest polydispersity index
- Highest entrapment efficiency
- Highest drug loading
- Most favourable zeta potential
- Greatest cumulative drug release after 12 hours

Based on these responses, SH9 was selected as the optimized formulation for subsequent in vitro drug release, release kinetic analysis, and stability evaluation.

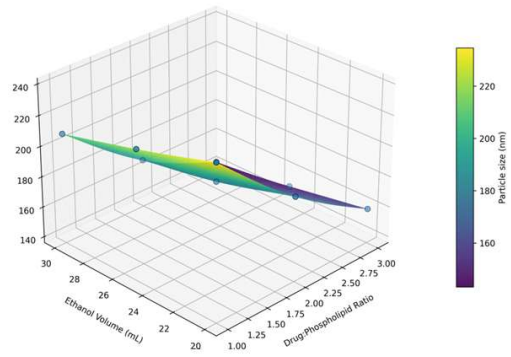

Figure 4A. Response surface plot illustrating the effect of drug-to-phospholipid ratio and ethanol volume on particle size of silymarin herbosomes.

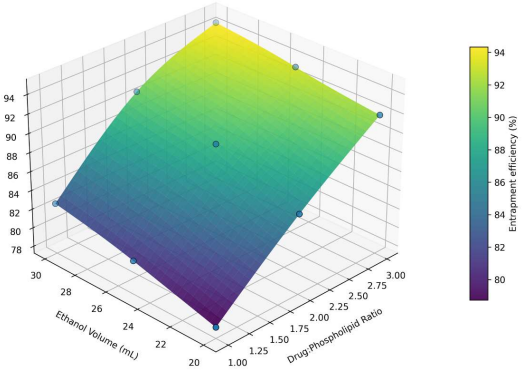

Figure 4B. Response surface plot illustrating the effect of drug-to-phospholipid ratio and ethanol volume on entrapment efficiency of silymarin herbosomes.

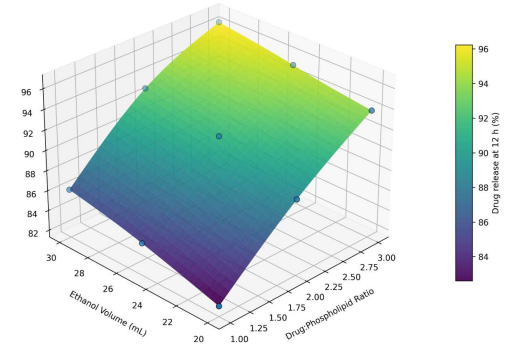

Figure 4C. Response surface plot illustrating the effect of drug-to-phospholipid ratio and ethanol volume on cumulative drug release of silymarin herbosomes after 12 h.

3.12 In Vitro Drug Release

The in vitro release profiles of pure silymarin and the prepared herbosomal formulations were evaluated using the dialysis bag diffusion method in phosphate buffer (pH 7.4) containing 0.5% Tween 80 at 37 ± 0.5 °C. The release profiles demonstrated that herbosomal formulations exhibited significantly improved dissolution characteristics compared with pure silymarin. Pure silymarin showed a slow dissolution pattern because of its poor aqueous solubility, achieving only 51.8 ± 1.4% cumulative drug release after 12 h. In contrast, all herbosomal

formulations exhibited enhanced release, ranging from 82.3 ± 1.6% for SH1 to 96.3 ± 0.6% for SH9. The enhanced dissolution may be attributed to the formation of a molecular complex between silymarin and phosphatidylcholine, reduced particle size, increased surface area, and improved wettability of the drug. These factors collectively facilitated faster penetration of the dissolution medium into the formulation and improved diffusion of silymarin across the dialysis membrane. The optimized formulation (SH9) exhibited a controlled release pattern characterized by an initial moderate release during the first two hours, followed by sustained drug release up to 12 h. Such behaviour is desirable because it may help maintain prolonged drug availability while avoiding rapid depletion of the entrapped drug.

Table 2. Cumulative drug release profile

Time (h)	Pure Silymarin (%)	SH9 (%)
0.5	6.2 ± 0.5	15.4 ± 0.6
1	10.4 ± 0.7	27.8 ± 0.8
2	18.7 ± 0.9	44.6 ± 1.0
4	28.6 ± 1.1	63.9 ± 0.9
6	36.8 ± 1.3	77.8 ± 0.8
8	43.5 ± 1.4	87.4 ± 0.7
10	48.1 ± 1.5	92.4 ± 0.6
12	**51.8 ± 1.4**	**96.3 ± 0.6**

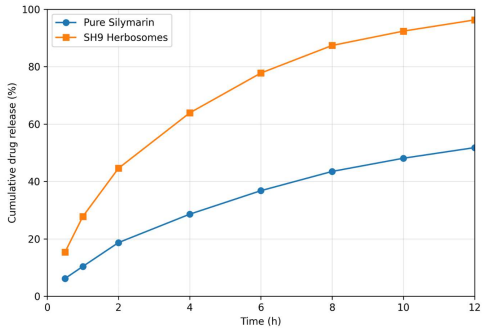

Figure 7. Comparative in vitro drug release profiles of pure silymarin and the optimized silymarin herbosomal formulation (SH9).

3.13 Drug Release Kinetic Analysis

The release data of the optimized herbosomal formulation were fitted to various kinetic models to identify the predominant mechanism of drug release. The regression coefficients (R^2) obtained for each model are presented below.

Table 3. Release kinetic analysis

Model	R^2
Zero-order	0.963
First-order	0.972
Higuchi	0.989
Korsmeyer–Peppas	**0.995**
Hixson–Crowell	0.978

The results indicated that the Korsmeyer–Peppas model provided the best fit for the release profile (R^2 = 0.995), suggesting that drug release was governed predominantly by diffusion through the phospholipid matrix. The release exponent (n = 0.61) indicated anomalous (non-Fickian) transport, implying that both diffusion of silymarin and gradual relaxation of the phospholipid matrix contributed to the overall release process. This behaviour is consistent with phospholipid-based delivery systems, where molecular diffusion and matrix restructuring occur simultaneously.

3.14 Accelerated Stability Study

The optimized herbosomal formulation (SH9) was subjected to accelerated stability testing for three months. No evidence of phase separation, precipitation, colour change, or aggregation was observed throughout the storage period. Only minor changes were noted in particle size, entrapment efficiency, and cumulative drug release, indicating good physicochemical stability.

Table 4. Stability study of SH9

Parameter	Initial	3 Months
Particle size (nm)	142.8 ± 2.1	148.2 ± 2.6
PDI	0.187 ± 0.01	0.196 ± 0.01
Zeta potential (mV)	−37.8 ± 0.5	−36.9 ± 0.7
Entrapment efficiency (%)	94.4 ± 0.5	92.8 ± 0.7
Drug loading (%)	12.4 ± 0.2	12.0 ± 0.2
Drug release (12 h, %)	96.3 ± 0.6	94.8 ± 0.8

The slight increase in particle size may be attributed to limited particle interaction during storage, whereas the small reduction in entrapment efficiency could result from gradual diffusion of a small fraction of entrapped drug from the phospholipid matrix. Nevertheless, the observed changes were minimal and did not substantially affect the overall performance of the formulation. The retention of a highly negative zeta potential throughout the storage period further supports the physical stability of the optimized herbosomal system by minimizing particle aggregation.

3.15 Overall Discussion

The findings demonstrate that the solvent evaporation method is suitable for preparing nanosized silymarin herbosomes with favourable physicochemical properties. Optimization of the drug-to-phospholipid ratio and ethanol volume significantly influenced particle size, entrapment efficiency, and drug release. Among the formulations, SH9 consistently showed the most desirable characteristics, including the smallest particle size (142.8 nm), narrow particle size distribution (PDI 0.187), high entrapment efficiency (94.4%), high drug loading (12.4%), and sustained drug release (96.3% at 12 h). The FTIR and DSC analyses supported successful molecular complex formation between silymarin and phosphatidylcholine without evidence of chemical incompatibility. SEM observations indicated uniform, spherical particles with minimal aggregation, while release kinetic modelling suggested anomalous diffusion-controlled release from the phospholipid matrix. Overall, these results illustrate how phospholipid complexation can

enhance the pharmaceutical performance of silymarin by improving dispersion, dissolution, and formulation stability.

4. Conclusion

The present study demonstrated the feasibility of developing silymarin-loaded herbosomes using the solvent evaporation technique and optimizing the formulation through a Quality by Design approach. The optimization indicated that both the drug-to-phospholipid ratio and ethanol volume markedly influenced particle size, entrapment efficiency, and drug release characteristics. Among the formulations, SH9 exhibited the most favourable physicochemical properties, including nanosized particles, a narrow size distribution, high entrapment efficiency, excellent drug loading, and sustained in vitro drug release. The FTIR and DSC analyses suggested successful molecular complexation between silymarin and phosphatidylcholine without evidence of chemical incompatibility, while SEM indicated uniform spherical particles with minimal aggregation. The optimized formulation also demonstrated good stability under accelerated storage conditions and followed anomalous diffusion-controlled drug release kinetics. Overall, these findings illustrate the potential of herbosomal technology to overcome the poor aqueous solubility and limited pharmaceutical performance of silymarin.

Acknowledgements

The authors acknowledge the support provided by the Department of Pharmaceutics and the institutional research laboratory for providing the necessary facilities to conduct this work. The authors also thank the technical staff for their assistance during analytical and characterization studies.

Conflict of Interest

The authors declare that there is no conflict of interest regarding the publication of this work.

Funding

The authors declare that no external funding was received for this study.

References

Al-Samydai, A., Nsairat, H., Abu Hajleh, M. N., Aburas, B., Akour, A., Ata, T. H., Mahmood, T. H., Al-Sammarraie, T. R., Atta, R., Ali, R., Alazzawi, Q. K., Aburjai, A., & Carradori, S. (2025). Meta-analysis of nano-phytosomes: unleashing the potential of plant-derived compounds for advancing cancer therapy. *Nat Prod Res*, *39*(16), 4623-4642. https://doi.org/10.1080/14786419.2024.2344182

Alharbi, W. S., Almughem, F. A., Almehmady, A. M., Jarallah, S. J., Alsharif, W. K., Alzahrani, N. M., & Alshehri, A. A. (2021). Phytosomes as an Emerging Nanotechnology Platform for the Topical Delivery of Bioactive Phytochemicals. *Pharmaceutics*, *13*(9). https://doi.org/10.3390/pharmaceutics13091475

Bageorgou, F., Li, L., Beausillon, C., Stennevin, A., Ortiz-Brugués, A., & Saurat, J. H. (2023). Tolerability and effectiveness of a dermocosmetic product containing Silybum marianum fruit extract in adolescents and young adults with acne-prone skin: An international, phase IV, longitudinal study. *J Cosmet Dermatol*, *22*(8), 2259-2267. https://doi.org/10.1111/jocd.15705

Behuria, H. G., Biswal, B. K., & Sahu, S. K. (2021). Electroformation of liposomes and phytosomes using copper electrode. *J Liposome Res*, *31*(3), 255-266. https://doi.org/10.1080/08982104.2020.1800729

Biradar, P. R., Naik, S., Dwivedi, P. S. R., Mallur, R. S., Mole, S. S., & Hungund, B. (2026). Neuroprotective effects of Premna integrifolia nano-phytosomes in haloperidol-induced Parkinson's rat model: A computational-guided Olivil nanoformulation delivery approach. *Metabolic Brain Disease*, *41*(1). https://doi.org/10.1007/s11011-026-01821-z

Bjørklund, G., Storchylo, O., Butnariu, M., Dadar, M., & Chirumbolo, S. (2025). Milk Thistle (Silybum marianum): Potential Role in Cancer Prevention. *Curr Med Chem*, *32*(39), 8895-8912. https://doi.org/10.2174/0109298673371391250415105506

Chen, R. P., Chavda, V. P., Patel, A. B., & Chen, Z. S. (2022). Phytochemical Delivery Through Transferosome (Phytosome): An Advanced Transdermal Drug Delivery for Complementary Medicines. *Front Pharmacol*, *13*, 850862. https://doi.org/10.3389/fphar.2022.850862

Chettupalli, A. K., Bukke, S. P. N., Vardhan, J., Yadhav, S., Mamilla Mugaiahgari, B. K., Jahnavi, P., Yata, V. K., & Narapureddy, B. R. (2025). Polyherbal formulations and phytosome-based delivery in diabetic wound healing: an integrative review. *J Biomater Sci Polym Ed*, 1-28. https://doi.org/10.1080/09205063.2025.2568684

Dewi, M. K., Muhaimin, M., Joni, I. M., Hermanto, F., & Chaerunisaa, A. Y. (2024). Fabrication of phytosome with enhanced activity of Sonneratia alba extract: Formulation modeling and in vivo antimalarial study. *International Journal of Nanomedicine*, *19*, 9411-9435. https://doi.org/10.2147/IJN.S467811

Eita, A. A. B. (2022). Milk thistle (Silybum marianum (L.)Gaertn.): An overview about its pharmacology and medicinal uses with an emphasis on oral diseases. *J Oral Biosci*,

64(1), 71-76. https://doi.org/10.1016/j.job.2021.12.005

Giri, S., Pandey, V. R., Fatima, F., Saroj, B. K., Gupta, P. S., Rahamanulla, A., Hussain, Z., & Sharma, G. (2025). Development and Characterization of a Polyherbal Phytosome Containing a Herbal Blend of Azadirachta indica, Angelica sinensis Polysaccharides, and Aloe vera for Anticancer Activity. *Journal of Carcinogenesis 24*(7s), 481-492.

Gunjal, A. H., Chandola, H., Harisha, C. R., Shukla, V. J., Goyal, M., & Pandya, P. (2013). Pharmacognostical and Preliminary physicochemical evaluation of Triphaladi granules - A polyherbal Ayurvedic formulation. *Ayu*, *34*(3), 288-293. https://doi.org/10.4103/0974-8520.123128

Gupta, J., Verma, N., Wal, A., Panda, K. C., Yeleti, V. V., Singh, B., Mahajan, S., Kandhari, H., & Wal, P. (2025). Management of Steroid-Induced Diabetes: A Review of Herbal Medications and Their Role in Modulating Insulin Signaling Pathways. *Endocr Metab Immune Disord Drug Targets*. https://doi.org/10.2174/0118715303327497241214054628

Gyawali, D., Vohra, R., Orme-Johnson, D., Ramaratnam, S., & Schneider, R. H. (2021). A Systematic Review and Meta-Analysis of Ayurvedic Herbal Preparations for Hypercholesterolemia. *Medicina (Kaunas)*, *57*(6). https://doi.org/10.3390/medicina57060546

Hajibabaie, F., Abedpoor, N., Taghian, F., & Safavi, K. (2023). A Cocktail of Polyherbal Bioactive Compounds and Regular Mobility Training as Senolytic Approaches in Age-dependent Alzheimer's: the In Silico Analysis, Lifestyle Intervention in Old Age. *J Mol Neurosci*, *73*(2-3), 171-184. https://doi.org/10.1007/s12031-022-02086-8

Islam, N., Irfan, M., Hussain, T., Mushtaq, M., Khan, I. U., Yousaf, A. M., Ghori, M. U., & Shahzad, Y. (2022). Piperine phytosomes for bioavailability enhancement of domperidone. *J Liposome Res*, *32*(2), 172-180. https://doi.org/10.1080/08982104.2021.1918153

Kamini, & Puri, D. (2025). QbD assisted formulation, optimization and characterization of psoralen phytosome prepared through thin film hydration method. *Drug Development and Industrial Pharmacy*, *52*(2), 291-312. https://doi.org/10.1080/03639045.2025.2593532

Liava, V., Ntatsi, G., & Karkanis, A. (2023). Seed Germination of Three Milk Thistle (Silybum marianum (L.) Gaertn.) Populations of Greek Origin: Temperature, Duration, and Storage Conditions Effects. *Plants (Basel)*, *12*(5). https://doi.org/10.3390/plants12051025

Nawaz, A., Zaib, S., Khan, I., Ahmed, A., Shahzadi, K., & Riaz, H. (2023). Silybum marianum: An Overview of its Phytochemistry and Pharmacological Activities with Emphasis on Potential Anticancer Properties. *Anticancer Agents Med Chem*, *23*(13), 1519-1534. https://doi.org/10.2174/1871520623666230412111152

Randisi, F., Modoni, G., Riva, M., Perletti, G., Odorico, D., Marras, E., & Gariboldi, M. B. (2026). Silybum marianum-Derived Compounds in Prostate Cancer: Mechanisms of Action and Translational Potential. *Int J Mol Sci*, *27*(10). https://doi.org/10.3390/ijms27104605

Rath, P., Prakash, D., Ranjan, A., Chauhan, A., Jindal, T., Alamri, S., Alamri, T., Harakeh, S., & Haque, S. (2024). Modulation of Insulin Resistance by Silybum marianum Leaves, and its Synergistic Efficacy with Gymnema sylvestre, Momordica charantia, Trigonella-foenum graecum Against Protein Tyrosine Phosphatase 1B. *Biotechnol Genet Eng Rev*, *40*(4), 3805-3827. https://doi.org/10.1080/02648725.2022.2162236

Shaker, M. K., Hassany, M., Eysa, B., Adel, A., Zidan, A., & Mohamed, S. (2025). The activity of a herbal medicinal product of Phyllanthus niruri and Silybum marianum powdered extracts (Heptex®) in patients with apparent risk factors for nonalcoholic steatohepatitis: a phase II, multicentered, randomized, double-blind, placebo-controlled clinical trial. *BMC Complement Med Ther*, *25*(1), 8. https://doi.org/10.1186/s12906-024-04692-y